Electronic Supplementary Material (ESI) for CrystEngComm.

Trends in Rare Earth Thiophosphate Syntheses: $Rb_3Ln(PS_4)_2$ (Ln = La, Pr, Ce), $Rb_{3-x}Na_xLn(PS_4)_2$ (Ln = Pr, Ce; x = 0.50, 0.55), and $RbEuPS_4$ Obtained by Molten Flux Crystal Growth.

Logan S. Breton, Mark D. Smith, Hans-Conrad zur Loye*

Department of Chemistry and Biochemistry, University of South Carolina, Columbia, South Carolina 29208, United States

*zurLoye@mailbox.sc.edu

Table of Contents

1. Phase pure $RbEuPS_4$ PXRD

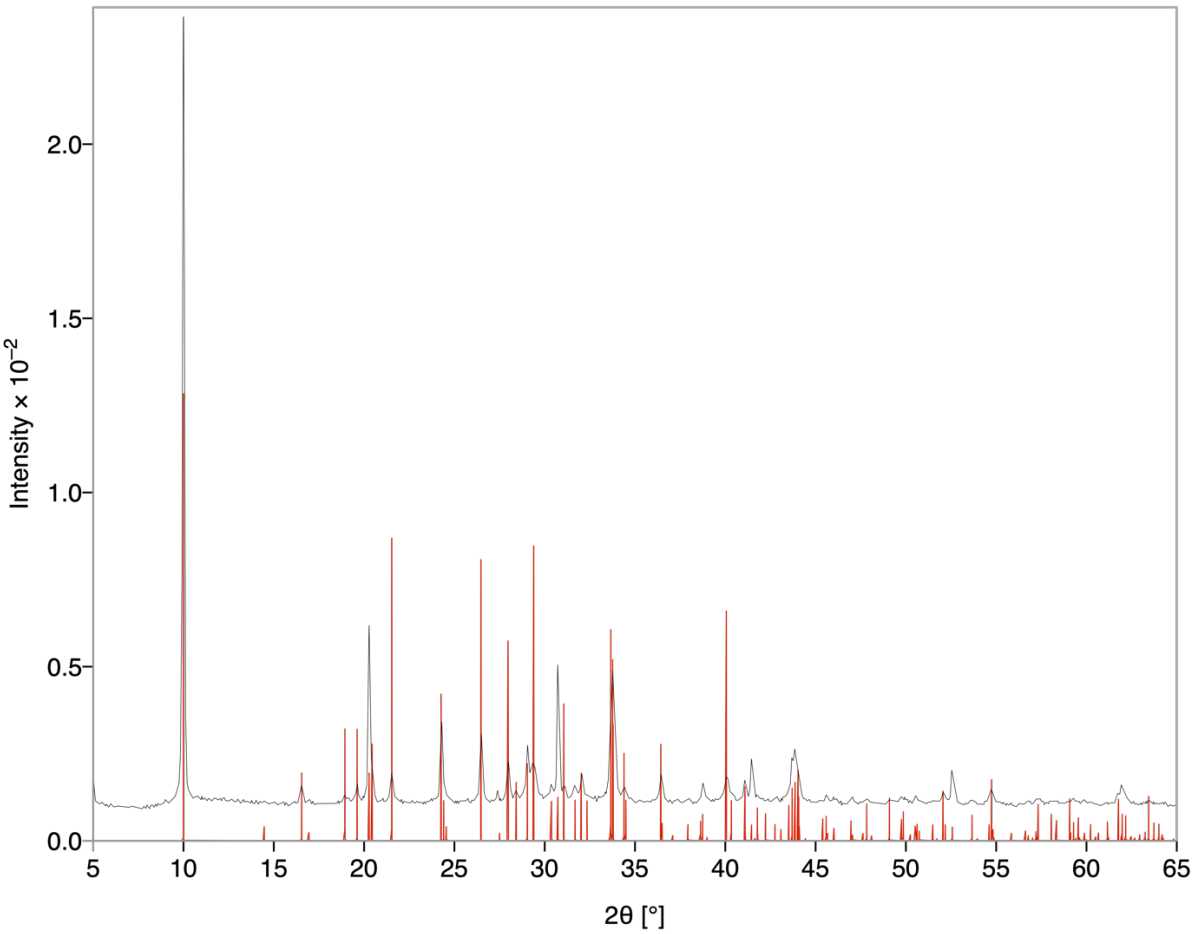

Figure S1. PXRD pattern of phase pure $RbEuPS_4$.

2. SEM Images

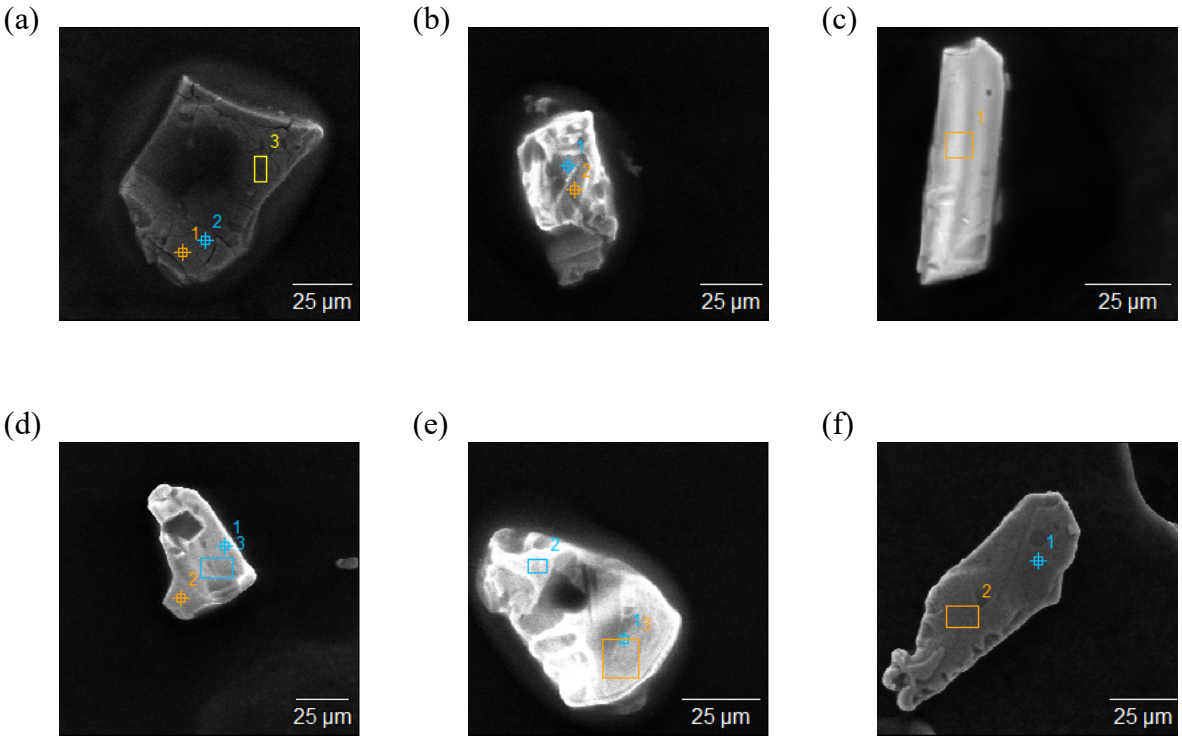

Figure S2. SEM images of (a) $Rb_3La(PS_4)_2$, (b) $Rb_3Ce(PS_4)_2$, (c) $Rb_3Pr(PS_4)_2$, (d) $Rb_{2.45(2)}Na_{0.55(2)}Pr(PS_4)_2$, (e) $Rb_{2.50(6)}Na_{0.50(6)}Ce(PS_4)_2$, (f) $RbEuPS_4$.

3. SEM Spectra

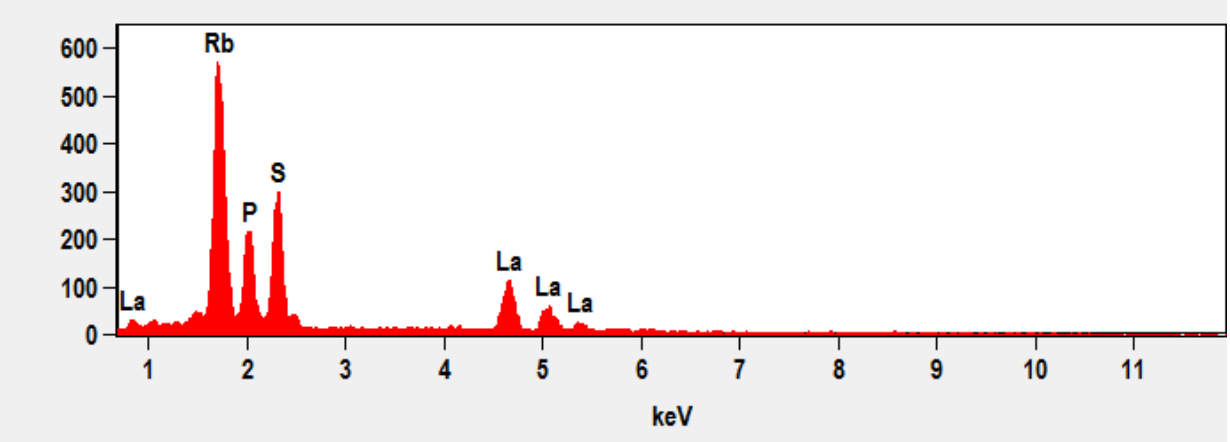

Figure S3. EDS spectrum of $Rb_3La(PS_4)_2$.

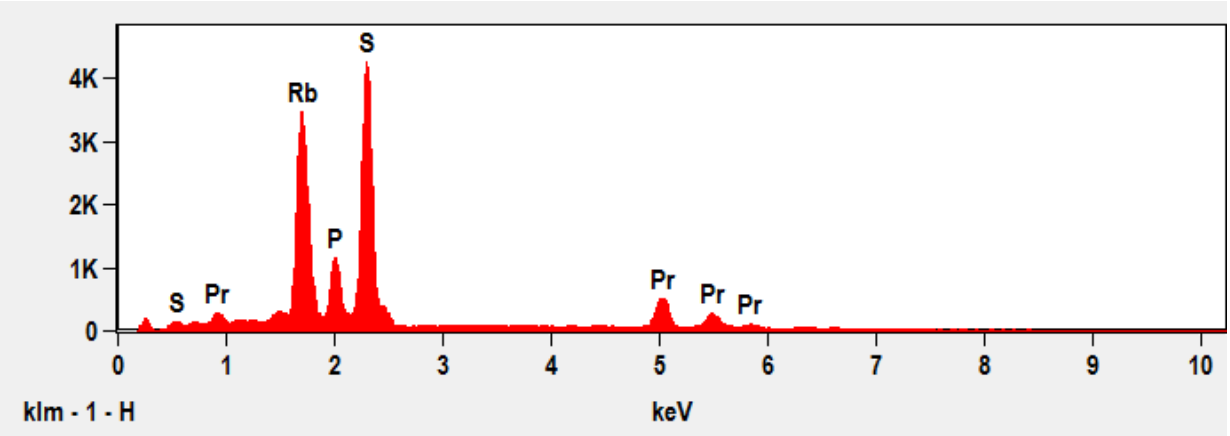

Figure S4. EDS spectrum of $Rb_3Pr(PS_4)_2$.

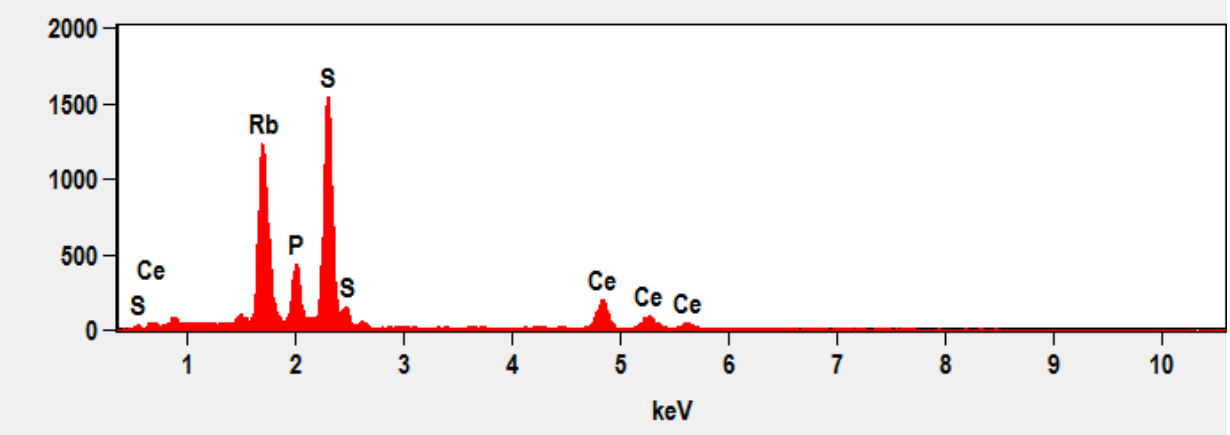

Figure S5. EDS spectrum of $Rb_3Ce(PS_4)_2$.

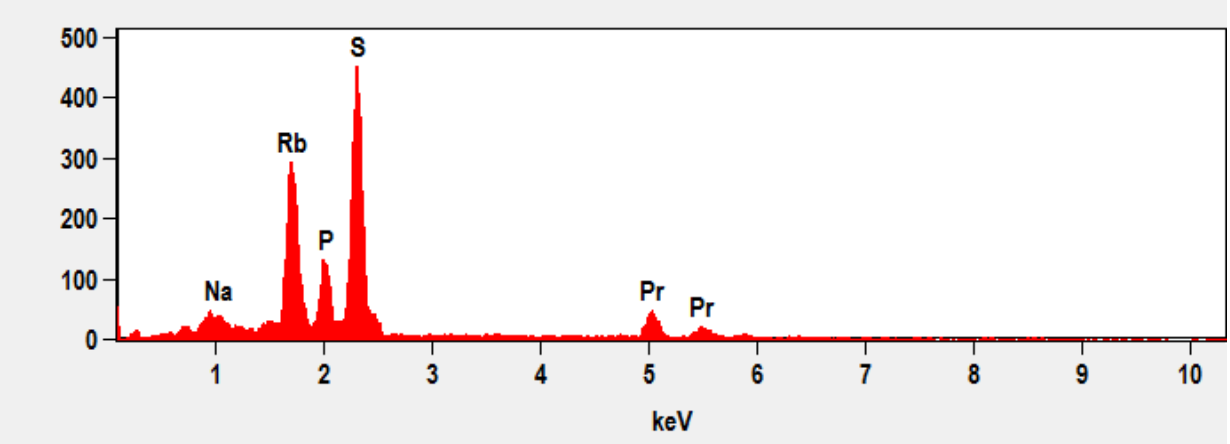

Figure S6. EDS spectrum of $Rb_{2.45(2)}Na_{0.55(2)}Pr(PS_4)_2$.

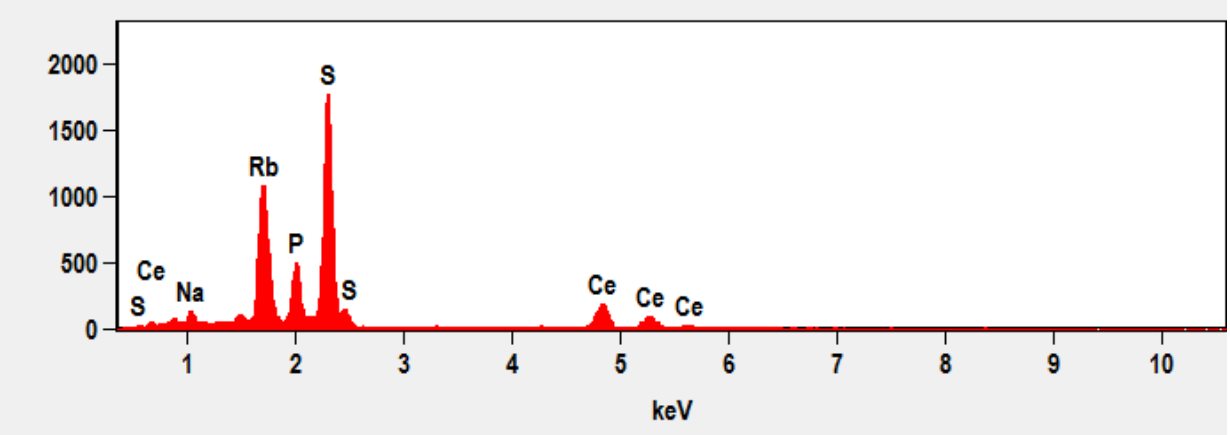

Figure S7. EDS spectrum of $Rb_{2.50(6)}Na_{0.50(6)}Ce(PS_4)_2$.

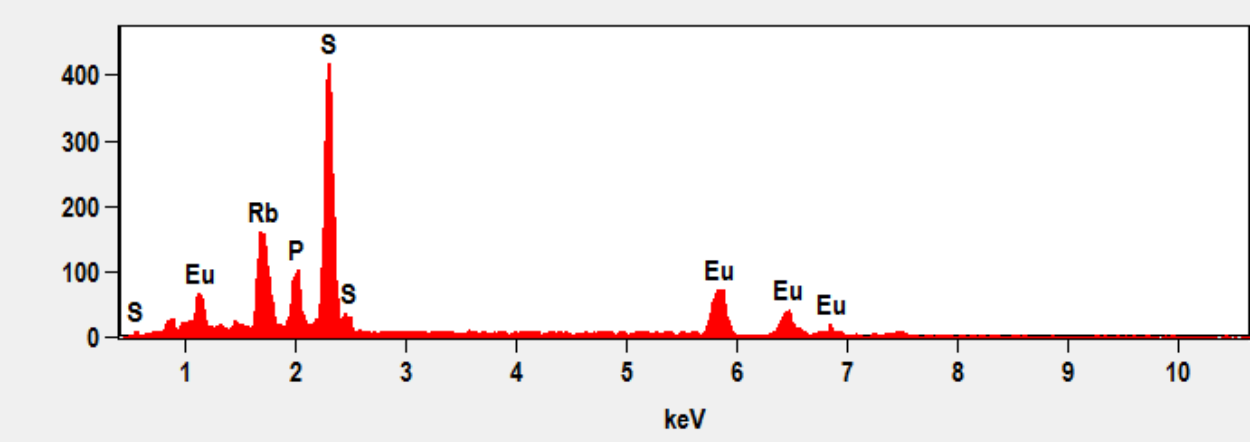

Figure S8. EDS Spectrum of $RbEuPS_4$.

4. Elemental Compositions

Table S1. Elemental compositions of the thiophosphates as determined by EDS.

$Rb_3La(PS_4)_2$		$Rb_3Pr(PS_4)_2$		$Rb_3Ce(PS_4)_2$	
Element	Atom %	Element	Atom %	Element	Atom %
Rb	27.92	Rb	19.54	Rb	19.33
La	12.88	Pr	7.93	Ce	7.76
P	23.61	P	15.95	P	14.18
S	35.59	S	56.59	S	58.55
$Rb_{2.45(2)}Na_{0.55(2)}Pr(PS_4)_2$		$Rb_{2.50(6)}Na_{0.50(6)}Ce(PS_4)_2$		$RbEuPS_4$	
Element	Atom %	Element	Atom %	Element	Atom %
Rb	15.61	Rb	16.05	Rb	13.42
Na	3.66	Na	3.6	Eu	12.13
Pr	6.29	Ce	7.37	P	14.48
P	15.11	P	14.92	S	59.98
S	59.33	S	58.06		

5. Detailed explanations of X-Ray structure determination

a) $Rb_3Ln(PS_4)_2$ (Ln = La, Ce, Pr)

X-ray intensity data from small irregular crystals were collected at 301(2) K for $Rb_3Ln(PS_4)_2$ (Ln = Pr, Ce) and at 291(2) K for $Rb_3La(PS_4)_2$ using a Bruker D8 QUEST diffractometer equipped with a PHOTON-II area detector and an Incoatec microfocus source (Mo Kα radiation, λ = 0.71073 Å). The raw area detector data frames were reduced and corrected for absorption effects using the SAINT+ and SADABS programs.[1, 2] Final unit cell parameters were determined by least-squares refinement of large sets of reflections taken from each data set. An initial structural model was obtained with SHELXT.[3] Subsequent difference Fourier calculations and full-matrix least-squares refinement against F^2 were performed with SHELXL-2018[4] using the ShelXle interface.[5]

The compounds crystallize in the monoclinic system. The pattern of systematic absences in the intensity data was consistent with the monoclinic space groups $P2_1$ and $P2_1/m$. Both space groups were investigated, and the best solution was obtained in $P2_1$, though the structures are pseudosymmetric (see below). The asymmetric unit in $P2_1$ consists of one lanthanide (Ln) atom, three Rb atoms, two P and eight unique S atoms. All atoms are located on positions of general crystallographic symmetry (site 2*a*). Unique to the Ln = La structure, two sites (La1/Rb1 and La2/Rb2) were modeled as mixed La/Rb sites after trial refinements showed either a significant decrease from full La occupancy or an increase from full Rb occupancy on these sites. The Rb3 and Rb4 sites refined to 100% rubidium within error. The presence of the smaller La^{3+} ion on these two sites but not on the Rb3 and Rb4 sites also correlates with the shorter observed La1/Rb1-S and La2/Rb2-S bond distances compared to Rb3-S and Rb4-S. The La/Rb occupancy values of each mixed site were constrained to sum to 100%, and the occupancies were further restrained to sum to one Rb and one La distributed over two sites, in order to satisfy crystal charge balance. Site occupancies refined to La1/Rb1 = 0.548(4)/0.452(4) and La2/Rb2 = 0.452(4)/0.548(2). Free refinement of the occupancies gave a composition near the final one, *i.e.* "$Rb_{3.1}La_{0.9}$". Trial refinements of the metal site occupation factors in the Ln = Ce and Pr structures showed no significant deviations from full occupancy. In the Ln = Ce and Pr structures, one sulfur atom (S4) showed a prolate displacement ellipsoid, along with significant electron density *ca*. 0.75 Å from

the site with a similar P-S distance as the main S4 site. This peak was interpreted as arising from a split S4 position, S4A/S4B. For Ln = Ce, refinement as a disordered S4 site improved the data/model agreement from $R1/wR2 = 0.029/0.056$ to 0.026/0.052 and flattened the difference map from +1.38/-0.90 to +0.77/-0.72 $e^-/Å^3$. A similar improvement was achieved for Ln = Pr. The S4 occupancies refined to S4A/S4B = 0.67(2)/0.33(2) for Ln = Ce and S4A/S4B = 0.69(1)/0.31(1) for Ln = Pr. For Ln = La, S4 was better described as a single site as no change in *R*-factors or difference map features was observed. All atoms were refined with anisotropic displacement parameters. As suggested by the metric similarity to the orthorhombic system, the crystals were all pseudo-orthorhombic twins. The twin law (1 0 0 / 0 -1 0 / 0 0 -1) was included in the refinements. Additionally, each two-fold related twin domain is further twinned by inversion. The final refinement model therefore included contributions from four domains, with refined crystal volume fractions of: La, 0.28(4), 0.25(4), 0.26(4), 0.21(4); Ce, 0.38(2), 0.13(2), 0.37(2), 0.12(2); Pr, 0.40(2), 0.11(2), 0.37(3) and 0.12(2), The largest residual electron density peak and hole in the final difference map are: La, +1.99 and -1.68 $e^-/Å^3$, located 0.73 and 0.79 Å from S8 and Rb4, respectively; Ce, +0.77 and -0.72 $e^-/Å^3$, located 0.81 and 0.71 Å from Ce1 and Rb4, respectively, and Pr, +0.84 and -0.86 $e^-/Å^3$, both located 0.19 and 0.78 Å from Rb4.

Space group $P2_1$ or $P2_1/m$ (pseudosymmetry). Manual examination of the structures, along with the ADDSYM results, shows that most atomic positions determined in $P2_1$ are also consistent with the centrosymmetric space group $P2_1/m$. For Ln = Ce and Pr, a model in $P2_1/m$ refines well, giving $R1/wR2 = 0.027/0.054$ for Ln = Ce and 0.035/0.061 for Ln = Pr, *i.e.* negligibly inferior to the $P2_1$ refinements of each dataset. However, in $P2_1/m$ the disorder of one sulfur atom of one PS_4 tetrahedron, which was also observed in $P2_1$ as S4A/B, now occurs across a crystallographic mirror plane. This imposed mirror symmetry constrains the PS_4 component occupancies to exactly 50/50. The occupancies in $P2_1$ (based only on the single pair S4A/S4B) refined to S4A/S4B = 0.67(2)/0.33(2) for Ln = Ce and S4A/S4B = 0.69(1)/0.31(1) for Ln = Pr. $P2_1$ was therefore was chosen as the better description of the structure because it allows for refinement of the individual occupancies of the disordered PS_4 group (position S4A/B, subject to a full total occupancy constraint). The departure of the refined S4A/B site occupancy from 50/50, though very small, is apparently genuine and therefore justifies the adoption of the acentric $P2_1$ over $P2_1/m$, and the categorization of these structures as pseudosymmetric. For Ln = La, solution and refinement in different space groups and crystal systems (*e.g.* $P2_1/m$, $P2_12_12_1$, *Pnma*) were not successful. All

resulted in high *R*-factors ($R1 > 10\%$), and larger difference map extrema than from the $P2_1$ model. It is not obvious why $P2_1$ gives the superior statistics, but it appears to be because of the cumulative effect of many slight atomic position deviations from consistency with higher symmetry. This subtle effect in manifested in a larger average displacement parameter observed in the higher space groups (*e.g.* 0.052 Å^2 for $P2_1/m$ vs 0.043 Å^2 for $P2_1$), suggesting small positional displacements from the average sites in high symmetry groups which are resolved in $P2_1$.

b) $Rb_{2.55(1)}Na_{0.45(1)}Pr(PS_4)_2$

X-ray intensity data from an irregular colorless crystal were collected at 100(2) K using a Bruker D8 QUEST diffractometer equipped with a PHOTON-II area detector and an Incoatec microfocus source (Mo Kα radiation, λ = 0.71073 Å). The data collection covered 100% of reciprocal space to $2\theta_{max} = 60.0^o$, with an average reflection redundancy of 10.8 and $R_{int} = 0.046$ after absorption correction. The raw area detector data frames were reduced and corrected for absorption effects using the SAINT+ and SADABS programs. [1, 2] Final unit cell parameters were determined by least-squares refinement of 9872 reflections taken from the data set. An initial structural model was obtained with SHELXT. [3] Subsequent difference Fourier calculations and full-matrix least-squares refinement against F^2 were performed with SHELXL-2018[4] using the ShelXle interface. [5]

The compound crystallizes in the monoclinic system. The space group $P2_1/c$ was uniquely determined by the pattern of systematic absences in the intensity data and was confirmed by structure solution. The asymmetric unit consists of one Pr atom, two pure Rb sites and one mixed Rb/Na site, two P atoms and eight unique S atoms. All atoms are all located on positions of general crystallographic symmetry (site 4*e*). Site Rb2 refined to significantly less than full occupancy (~66% Rb). For charge balance reasons, this site was refined as a disordered mixture of rubidium and sodium, as a Rb/vacancy model would violate crystal electroneutrality. The Rb/Na occupancies were constrained to sum to 100% and refined to Rb2/Na2 = 0.449(2)/0.551(2). If refined as a single site, rubidium atoms Rb1 and Rb3 both displayed strongly prolate displacement parameters (U_3/U_1 = 5.1 for Rb1 and 7.3 for Rb3) with large satellite residual electron density peaks and holes (*ca*. +/-1.8 $e^-/Å^3$) located less than 0.5 Å from the main site. Split rubidium

positions better accounted for the observed electron density at both sites and reduced the *R*1-value by *ca*. 0.3% near convergence. The site occupancies refined to Rb1A/Rb1B = 0.936(9)/0.064(9) and Rb3A/Rb3B = 0.62(4)/0.38(4). All atoms were refined with anisotropic displacement parameters except for the minor Rb1 disorder components (Rb1B, isotropic). The largest residual electron density peak and hole in the final difference map are +0.87 and -1.23 $e^-/Å^3$, located 0.71 Å from Rb2/Na2 and 0.89 Å from S4, respectively.

c) $Rb_{2.50(1)}Na_{0.50(1)}Ce(PS_4)_2$

X-ray intensity data from a small needle were collected at 301(2) K using a Bruker D8 QUEST diffractometer equipped with a PHOTON-II area detector and an Incoatec microfocus source (Mo Kα radiation, λ = 0.71073 Å). The data collection covered 99.9% of reciprocal space to $2\theta_{max}$ = 56.6º, with an average reflection redundancy of 9.4 and R_{int} = 0.072 after absorption correction. The raw area detector data frames were reduced and corrected for absorption effects using the SAINT+ and SADABS programs. [1, 2] Final unit cell parameters were determined by least-squares refinement of 8427 reflections taken from the data set. An initial structural model was obtained with SHELXT.[3] Subsequent difference Fourier calculations and full-matrix least-squares refinement against F^2 were performed with SHELXL-2018[4] using the ShelXle interface. [5]

The compound crystallizes in the monoclinic system. The space group $P2_1/c$ was uniquely determined by the pattern of systematic absences in the intensity data and was confirmed by structure solution. The asymmetric unit consists of one cerium atom, two pure Rb sites and one mixed Rb/Na site, two P atoms and eight unique S atoms. All atoms are all located on positions of general crystallographic symmetry (site 4*e*). Site Rb2 refined to significantly less than full occupancy (~68% Rb). For charge balance reasons, this site was refined as a disordered mixture of rubidium and sodium, as a Rb/vacancy model would violate crystal electroneutrality. The Rb/Na occupancies were constrained to sum to 100%, and refined to Rb2/Na2 = 0.501(6)/499(6). If refined as a single site, rubidium atoms Rb1 and Rb3 both displayed strongly prolate displacement parameters. Split rubidium positions better accounted for the observed electron density at both sites, and reduced the *R*1-value by *ca*. 0.4% near convergence. The site occupancies refined to Rb1A/Rb1B = 0.955(14)/0.045(14) and Rb3A/Rb3B = 0.60(8)/0.40(8). All atoms were refined with anisotropic displacement parameters except for the minor disorder component Rb1B

(isotropic). The largest residual electron density peak and hole in the final difference map are +1.96 and -1.40 $e^-/Å^3$, located 0.91 Å and 0.83 Å from Ce1, respectively.

d) $RbEuPS_4$

X-ray intensity data from plate crystals were collected at 301(2) K using a Bruker D8 QUEST diffractometer equipped with a PHOTON-II area detector and an Incoatec microfocus source (Mo Kα radiation, λ = 0.71073 Å). The raw area detector data frames were reduced and corrected for absorption effects using the SAINT+ and SADABS programs.[1, 2] Final unit cell parameters were determined by least-squares refinement of large sets of reflections taken from each data set. An initial structural model was obtained with SHELXT.[3] Subsequent difference Fourier calculations and full-matrix least-squares refinement against F^2 were performed with SHELXL-2018[4] using the ShelXle interface.[5]

The compound $RbEuPS_4$ crystallizes in the orthorhombic crystal system. The space group *P*nma was uniquely determined by the pattern of systematic absences in the intensity data and was confirmed by structure solution. The asymmetric unit consists of one europium atom, three unique sulfur atoms, one phosphorus atom, and one disordered rubidium site. All atoms are located on positions of general crystallographic symmetry (site 8*d*). If refined as a single site, rubidium atom Rb1displayed a strongly prolate displacement parameter. Split rubidium positions better accounted for the observed electron density. The site occupancies refined to Rb1A/Rb1B = 0.261(17)/0.739(17). All atoms were refined with anisotropic displacement parameters. The largest residual electron density peak and hole in the final difference map are +1.18 and -1.0 $e^-/Å^3$, located 0.47 Å from Eu1 and 0.43 Å from Rb1B, respectively.

6. References

(1) L. Krause, R. Herbst-Irmer, G. M. Sheldrick, and D. Stalke, *J. Appl. Crystallogr.*, 2015, **48**, 3-10

(2) APEX3 Version 2019.1-0 and SAINT+ Version 8.40A., 2019, Bruker Nano, Inc., Madison, WI, United States.

(3) G. M. Sheldrick, *Acta Crystallogr. A*, 2015, **71**, 3-8

(4) G. M. Sheldrick, *Acta Crystallogr. A*, 2008, **64**, 112-122

(5) O. V. Dolomanov, L. J. Bourhis, R. J. Gildea, J. A. K. Howard, and H. Puschmann, *J. Appl. Crystallogr.*, 2009, **42**, 339-341